International Journal of Advanced Science and Research
ISSN: 2455-4227
Impact Factor: RJIF 5.12
www.allsciencejournal.com
Volume 2; Issue 5; September 2017; Page No. 143-148

Interferometers of synthetic aperture radar (InSAR) relevance in generation of digital elevation model (DEM) for real world solutions

Dr. Madan Mohan
Associate Professor of Geography, Centre for Study of Regional Development, School of Social Sciences – III, Jawaharlal Nehru University, New Delhi, India

Abstract
InSAR is a system based on microwave of electromagnetic spectrum of remote sensing. An active remote sensing system are as Shuttle Radar Topographic Mission and Radarsat satellites. These satellites have specific application in natural phenomena measurements as geophysical deformations studies – topography, surface changes/ tectonic deformation, volcanic eruption, land subsidence, landslides and so on displacements of earth surface. Likewise, microwave sensing has also significant role in infrastructure and building monitoring, bridge movement, tunnel deformation measurement as an early warning system. So, InSAR imagery are also used in generation of DEM which can help better understand and mange real world's problems in real time.

Keywords: microwave remote sensing, InSAR interferometry, geophysical deformation, DEM generation

1. Introduction

The Synthetic Aperature Radar (SAR) systems are used to record both the amplitude and the phase of backscattered echoes. It is perceived that the phase spectrum of an image is more characteristic to the image than its magnitude spectrum (Ghiglia and Pritt, 1998). So, the phase of each pixel of a focused SAR image is the sum of three distinct contributions as firstly, the two-ways path (sensor-target-sensor) divided by the used radar wavelength (which is in few centimetres) corresponds to millions of cycles; secondly, the interaction between the incident electromagnetic waves and then scatters within the ground resolution cell; and thirdly, the phase shift made by the processing system used to focus the image. However, the two SAR images from slightly different viewing angles are considered for interference, of which phase difference is used efficiently to generate digital elevation models (DEMs). The DEMs are utilised to monitor terrain changes and to measure minute surface displacements and for various purposes as environmental, hydrology, settlements and so on for solutions of the real world.

The Interferometers of Synthetic Aperture Radar (InSAR) is the "measurements of certain parameter such as the topography, surface change, and surface displacement from the interference of phase of two or more SAR acquisition over the same area". So, the term interfereogram define as the "the phases of two SAR images of the same area are made to interfere to generate an interferogarm having a number of interference fringe". Each interference fringe corresponds to a phase difference of 2π between the two component SAR images.

The interferogram is the complex product of two components of SAR images. These two SAR images can be taken simultaneously with the help of aircraft or satellite with two antenna separated by distance which is known as baseline. In other words, the Baseline is defined as "an aircraft/ satellite with two antenna separated by a distance known as baseline". So, the baseline is referred to as single pass or single track interferometry in which the "two SAR images are acquired in two different passes of the same satellite". On the other hand, the "Repeat Pass Interferometry" is referred to the "two different satellite, SAR images, revolving along more or less the same orbit with certain time difference".

2. SAR Interferometer Satellites

1. Single Pass
   SRTM = Shuttle Radar Topographic Mission, USA, NIMI, & NASA – 11 Days (11 to 22 February 2000).
2. Repeat Pass
   ERS-1, ERS-2 & JERS-1 (archived), RADARSAT-1 (functional), ENVISAT

3. Interferometer SAR Data Structure

1. Single Look Complex or SLC format
   Each pixel in SLC format is represented by equation given below:

$$a + ib$$

Now, Amplitude = $\sqrt{a^2 + b^2}$, Phase = $\tan^{-1} \frac{b}{a}$

On the one hand, for each pixel, 'a' and 'b' together occupy 8 bytes (4 bytes each) in case of complex float format or 4 bytes (2 bytes each) in case of complex integer format. It is usually supplied by NRSC Data Centre, India. On the other hand, in case of standard data, each pixel may be symbolised by a single character i.e., just one byte for an averaged multi look data. This shows the enormity in the size of interferometric data in contrast to standard data products.

4. Mathematical Background

i) Basic Geometry of SAR Interferometers

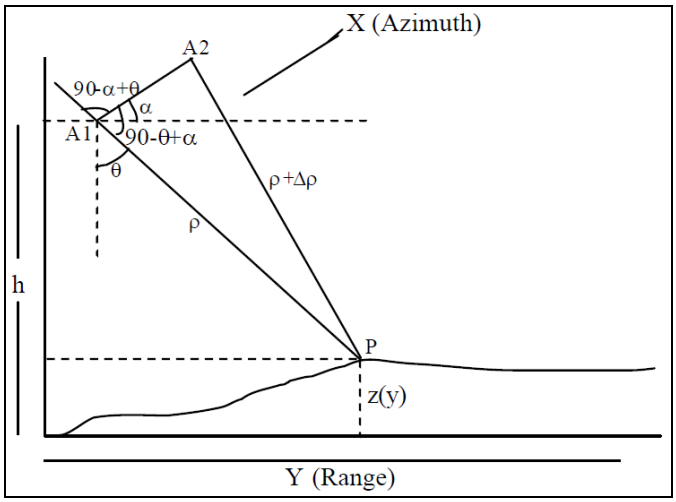

Fig 1: Elementary Geometry of SAR Interferometry. A1 and A2 represent 2 antenna viewing the similar surface.

ii) Geometry of Differential SAR Interferometry (D-InSAR)

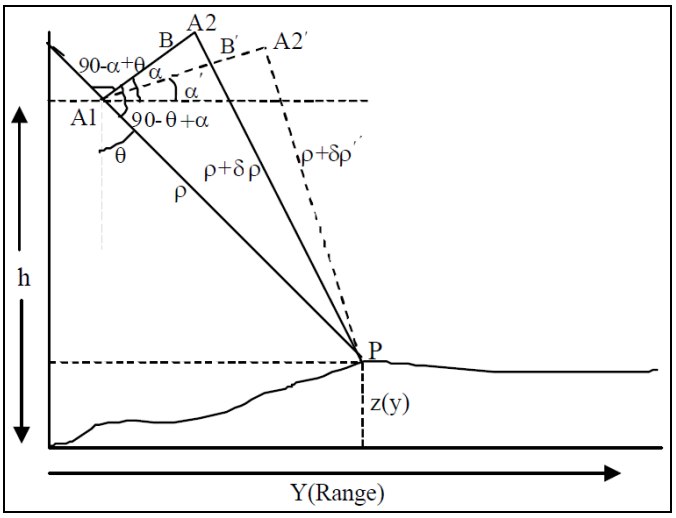

Fig 2: Elementary Geometry of Differential SAR Interferometry (D-InSAR). A2 and A2' represent 3 antenna viewing the identical surface. Data acquired from A1 and A2 are for measuring the topographic phase. From A2 and A2' (before and after the event) used for computing ground deformation.

5. Procedure for Generating Interferogram

1. Data Selection Baseline
   a. Spatial Baseline
   b. Temporal Baseline
2. Atmospheric Effects
   a. Cloud
   b. Haze
3. Orbital Deviation
   a. First Image Pair
      1) Spatial Baseline … 50 m to 300 m
      2) Temporal Baseline … 0
   b. Second Image Pair
      1) Spatial Baseline … 0

Master Image – one image of second pair may be common in first pair.

1) Data Processing

i) Generation of two interferogram
   a. Registration Accuracy 1/100th of a pixel
      (1) cross correlation of two amplitudes
      (2) Maximum value of coherence
      (3) Maximum signal to noise ratio in fringe spectrum
      (4) Minimization of average fluctuation of phase difference

ii) Extraction of phase component

2) DEM Generation

i) Flattening

$$\emptyset = \frac{\left(\frac{4\pi}{\lambda}\right) * (\rho * B)}{\rho}$$

ii) Phase Unwrapping
   a. Path following algorithm
   b. Least square algorithm
      (1) Unweighted robust technique
      (2) Weighted least square technique
      (3) Picard iteration technique

$$\varphi = \emptyset_{wp} + 2\pi * n$$

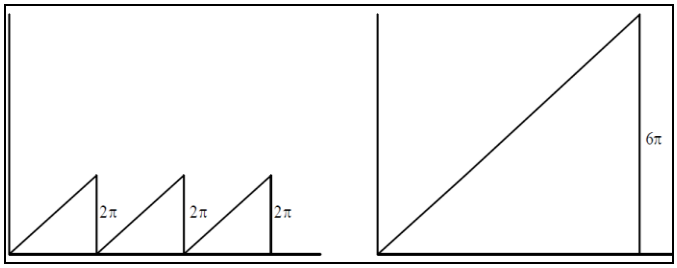

Fig 3: Model of phases: Wrapped phase (left); unwrapped actual phase (right).

iii) Determination of Absolute Phase

$$\emptyset abs = \emptyset up + \emptyset offset$$

iv) Phase to Height conversion
   a. Normal Baseline Model
   b. Integrated Incidence Angle Model
   c. Baseline Rotation Model

$$\Delta h = \frac{\lambda \rho \sin\theta}{4\pi * B \perp} * \Delta\theta$$

v) Extraction of Phase Component due to Surface Movements by D-InSAR Technique

$$\Delta\emptyset = \emptyset - (B \parallel B \parallel) * \emptyset$$

Subsequently,

$$\Delta\emptyset = \frac{4\pi}{\lambda} * \Delta\rho$$

DEM generation by SAR Interferometry Technique.

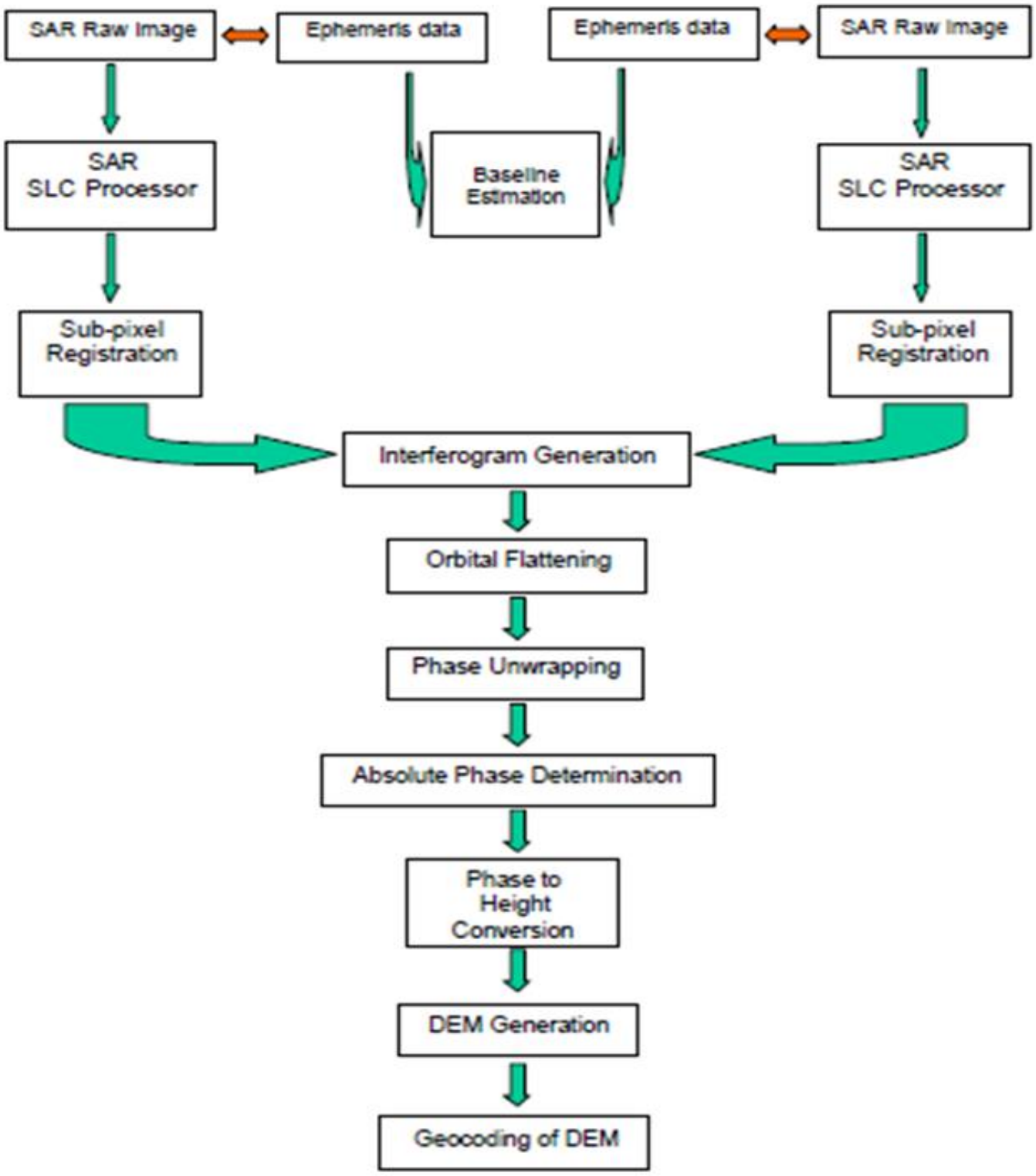

Fig 4: Step-by-step schematic procedure for DEM generation by SAR interferometry technique.

3) InSAR Applications for Real World

i) High Resolution Digital Elevation Model (DEM)

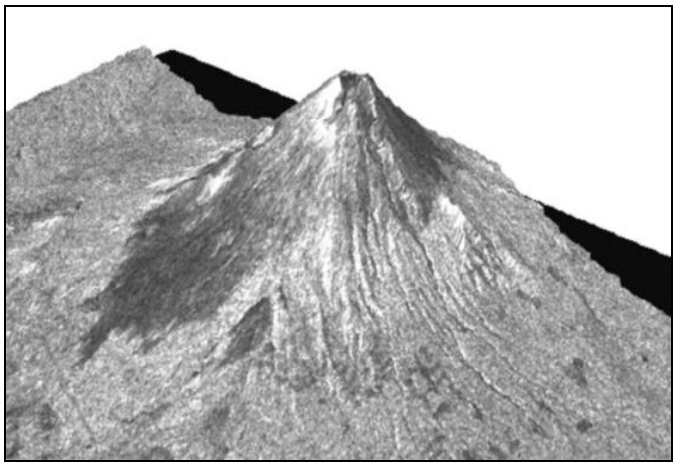

Fig 5: Digital Elevation Model (DEM) of Mt. Fuji, Japan derived from JERS-1 data. (*Image Curtsey:* NASDA/ EORC).

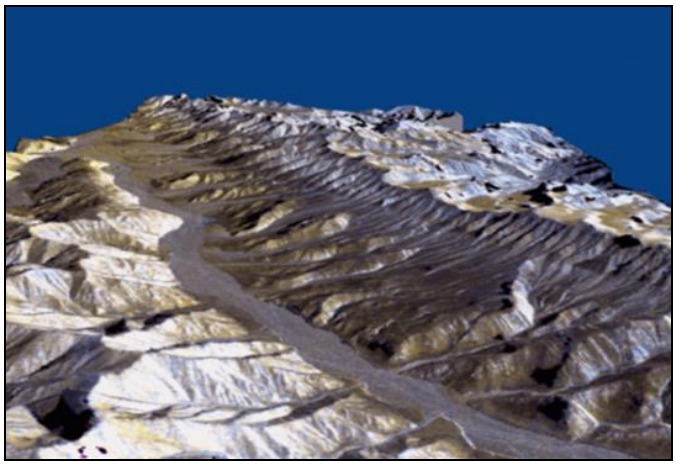

Fig 6: Landscape view of Karakax Valley, Northern Tibet derived from SIR-C Interferometric DEM and SIR-C imagery. (L-band: Red, L+C: Green, and C-band: Blue).

ii) Earthquake/ Crusted Deformation Studies

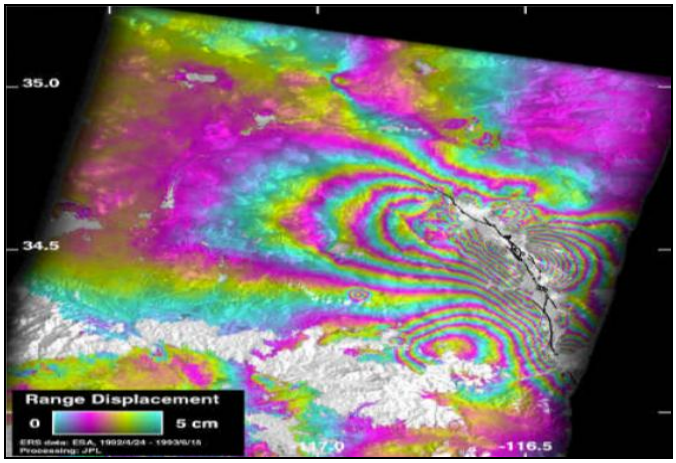

Fig 7: Differential interferogram (D-InSAR) use to present the co-seismic displacements of Landers Earthquake, California, USA (June 28, 1992; Mw = 7.3). It also depicts the loci of the rupture planes. The earthquake caused a surface break of ~ 70 km long with up to 6.2 m of right-lateral offset as is evidenced above.

iii) Volcano Monitoring Studies

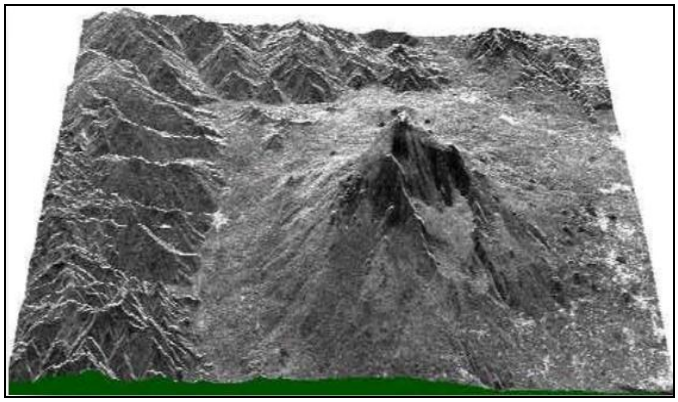

Fig 8: Digital Elevation Model (DEM) generated from ERS-1 and ERS-2 interferometric imagery pairs for the Mount Etna, Italy.

iv) Landslide Monitoring Studies

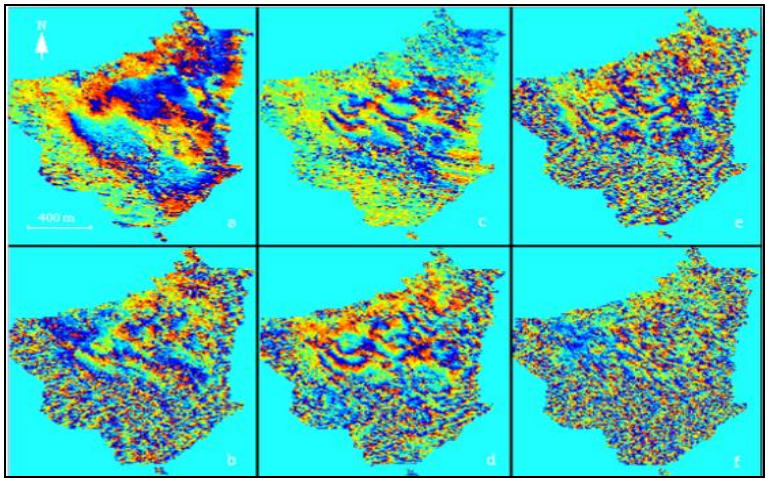

Fig 9: Digital analysis of the geocoded differential SAR interferograms (D-InSAR) showing line-of-sight displacement fringes of Saint-Etienne-de-Tinée landslide area located in the southern France.

v) Glacier Dynamics/ Ice Sheet Motion Studies

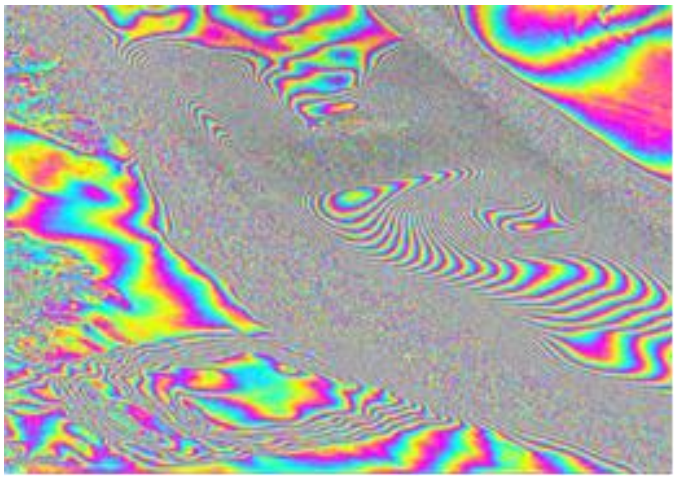

Fig 10: The Radar Interferogram used for the study of an area which includes a portion of the Rutford Ice Stream, Antarctica.

vi) Land Subsidence Studies

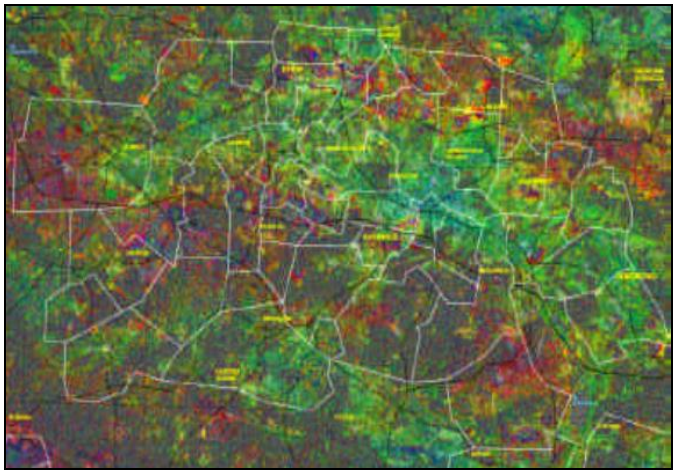

Fig 11: Differential SAR interferogram (D-InSAR) used for analysis of the patches of ground subsidence caused by underground coal mining during the period 04 Oct., 1992 to 08 Nov., 1992 in Upper Silesia, Poland.

6. Conclusions

Synthetic aperture radar (SAR) is a rational active microwave imaging system. In remote sensing it is used for modelling and mapping of the scattering properties of the Earth's surface in the respective wavelength domain of electromagnetic spectrum. Interferometric SAR (InSAR) studies the phase differences of at least two complex-valued SAR images obtained from different orbit positions, on one hand and at different times or periods, on the other hand. The information derived from these interferometric data sets can be practically applied to measure several geophysical quantities, such as topography, deformations (volcano monitoring studies, earthquake/ crusted deformation studies); ice sheets/fields motion studies: glacier dynamics - glacier flows; ocean currents; landslide monitoring studies, land subsidence studies; forest cover and vegetation properties, etc. with the help of generated Digital Elevation Model (DEM) for real world's problems and their solutions in real-time for the betterment of humanity.

7. References

1. Atkinson, Peter M, Tate Nicholas J. Advances in Remote Sensing and GIS Analysis, New Delhi, Wiley India Pvt. Ltd., 2013.
2. Bernstein R, Ferneyhough DG. Digital Image Processing, Photogrammetric Engineering, 1975; 41:1465-1476.
3. Blom RG, Daily M. Radar Image Processing for Rock Type Discrimination, IEEE Transactions on Geoscience and Remote Sensing, 1982; 20:343-351.
4. Bloom A, Fielding E, FU X. A Demonstration of Stereophotogrammetry with Combined SIR-B and Landsat TM images, International Journal of Remote Sensing, 1988; 9:1023-1038.
5. Buiten HJ, JGPW Clevers. Land Observation by Remote Sensing: Theory and Applications, in Gorden and Breach, Current Topics in Remote Sensing, 1993; 3:32-39.
6. Burgmann Roland, Paul A, Rosen, Eric J Fielding. Synthetic Aperture Radar Interferometry to Measure Earth's Surface Topography and its Deformation, Annual Review of Earth and Planetary Science, 2000; 28:169-209.
7. Campbell JB. Introduction to Remote Sensing, London, Taylor and Francis, 2007.
8. Camps-Valls G, Tuia D, Gómez-Chova L, Jiménez S, Malo J. Remote Sensing Image Processing, San Rafael, CA, Morgan and Claypool, 2011.
9. Jensen JR. Introductory Digital Image Processing: A Remote Sensing Perspective, Upper Saddle River, NY, Prentice Hall., 2005.
10. Kraak Menno-Jan, Ferjan Ormeling. Cartography: Visualization of Geospatial Data, New Delhi, Pearson Education Singapore Pte. Ltd., 2003.
11. Lillisand TM, Kiefer RW, Chipman JW. Remote Sensing and Image Interpretation, New Delhi, Wiley-INDIA John Wiley & Sons Asia Pte, Ltd. Fifth Edition, 2004.
12. Liu Jian Guo, Philippa JM. Essential Image Processing and GIS for Remote Sensing, Oxford, UK, John Wiley & Sons, Ltd., 2009.
13. Moik H. Digital Processing of Remotely Sensed Images, Washington D.C., NASA, Special No. 431, 1980.
14. Richards John A. Remote Sensing Digital Image Analysis: An Introduction, Heidlberg, New York Dordrecht, London, Springer, 2013.
15. Sabins Floyd F. Remote Sensing: Principles and Interpretation, Kolkata, Levant Books, 2013.

16. Scivier MS *et al*. Estimating SAR phase from complex SAR imagery, Journal of Physics D: Applied Physics, 1986; 19:357-362.
17. Shaw Gary A, Hsiao-hua K, Burke. Spectral Imaging for Remote Sensing, Lincoln Laboratory Journal. 2003; 14(1):3-28.
18. Zebker HA, Goldstein RM. Topographic Mapping from Interferometric Synthetic Aperture Radar Observations, Journal of Geophysics Research. 1986; 91(B5):4993-4999.